Science and Technology Indonesia
e-ISSN:2580-4391 *p*-ISSN:2580-4405
Vol. 11, No. 2, April 2026

Research Paper

Synthesis, In-Vitro Evaluation, and Computational Investigation of Salicylic Hydrazide Derivatives as Potential Tyrosine Kinase–Targeted Anticancer Agents

Melanny Ika Sulistyowaty[1,2*], Tri Widiandani[1,2], Albertus Aditya Setiawan[1,3], Seow Lay Jing[4], Neny Purwitasari[1], Ferlinahayati[5], Dwi Setyawan[1], Galih Satrio Putra[6,7], Anastasia Wheni Indrianingsih[8]

[1]*Department of Pharmaceutical Sciences, Faculty of Pharmacy, Universitas Airlangga, Surabaya, 60115, Indonesia*
[2]*Research Group of Drug Development, Faculty of Pharmacy, Universitas Airlangga, Surabaya 60115, Indonesia*
[3]*Pharmacist Professional Education Program, Faculty of Pharmacy, Universitas Hang Tuah, Surabaya, 60111, Indonesia*
[4]*Faculty of Pharmacy and Health Sciences, Universiti Kuala Lumpur, Royal College of Medicine Perak, Ipoh, 30450, Malaysia*
[5]*Department of Chemistry, Faculty of Mathematics and Natural Sciences, Universitas Sriwijaya, South Sumatra, 30662, Indonesia*
[6]*Department of Chemistry, Faculty of Mathematics and Natural Sciences, State University of Malang, Malang, 65145, Indonesia*
[7]*Graduate School of Engineering Science, The University of Osaka, Toyonaka, Osaka, 5608531, Japan*
[8]*Research Center for Food Technology and Processing, National Research and Innovation Agency (BRIN), Yogyakarta, 55861, Indonesia*
*__Corresponding author__: melanny-i-s@ff.unair.ac.id

Abstract
A series of N_2-acyl salicylic hydrazides (S2-S6) and N-(substituted benzylidene) salicylic hydrazides (S7-S9) were synthesized from 2-hydroxybenzohydrazide (S1), using both microwave irradiation and conventional methods, and tested for its in vitro anticancer activity against human lung cancer cell, A549. The salicylic hydrazides were successfully synthesized in good yields (79–98%) and the in-vitro study results indicated that 3,4-dichloro-N'-(2-hydroxybenzoyl)benzohydrazide (S5) was most active among the tested compounds (IC_{50} value of 68.75 μM). In this work, we applied an integrated approach combining network pharmacology and computational analysis to explore how salicylic hydrazide derivatives affect tyrosine kinase–related pathways. The in-silico findings were in agreement with the in vitro results, indicating that compound S5 produced a docking score of –6.53468 kcal/mol. The findings of this research are expected to support further development toward identifying promising anticancer drug candidates derived from salicylic hydrazide derivatives.

Keywords
Anticancer Drug Discovery, Microwave-Assisted Synthesis, Molecular Docking, Network Pharmacology, Salicylic Hydrazides, Tyrosine Kinase Inhibition

Received: 7 November 2025, Accepted: 25 February 2026
https://doi.org/10.26554/sti.2026.11.2.609-620

1. INTRODUCTION

Tyrosine kinases are pivotal regulators of various signaling pathways that control critical cellular functions, including proliferation, differentiation, and apoptosis (Sudhesh Dev et al., 2021). The aberrant activation of these kinases is a hallmark of many cancers, contributing to tumorigenesis and metastasis (Lian et al., 2019). Targeting tyrosine kinases has thus become a strategic approach in cancer therapy, with several inhibitors developed to combat resistant cancer phenotypes. As the understanding of these pathways evolves, the exploration of novel compounds that can effectively inhibit tyrosine kinase activity is crucial.

Salicylic hydrazide derivatives have emerged as promising candidates in the search for new anticancer agents. These compounds have been shown to influence multiple biological pathways, particularly those governing programmed cell death and the progression of the cell cycle, primarily through their influence on kinase signaling pathways (Altıntop et al., 2012). Recent studies suggest that salicylaldehyde derivatives may inhibit the activity of specific tyrosine kinases, thereby disrupting signaling cascades that are essential for cancer cell survival and proliferation. This potential opens avenues for their development as therapeutic agents in oncology (Nikolova-Mladenova et al., 2023).

Network pharmacology serves as a powerful integrative method to prioritize biological receptors for molecular docking studies, shifting from the traditional "one drug, one target" approach to a systems-level analysis of complex drug-disease interactions (Hopkins, 2008; Mutiah et al., 2024; Li and Kar, 2025). By mapping the relationships between a drug's bioac-

tive compounds, potential protein targets, and the associated disease pathways, this method identifies the key nodes within a biological network. These nodes represent the most functionally significant and therapeutically relevant receptors. Subsequently, detailed molecular docking simulations are performed on these prioritized targets to computationally validate the binding affinity and stability of the compounds, creating a rational pipeline from multi-target prediction to structural confirmation. This strategy significantly increases the likelihood of identifying meaningful pharmacological interactions.

For instance, network pharmacological analysis was employed to elucidate the therapeutic mechanisms of Curcuma species in osteosarcoma. The study identified several core protein targets-including AKT1, TNF, STAT3, EGFR, and HSP90AA1-that are critically involved in key oncogenic signaling pathways such as PI3K/Akt, HIF-1, ErbB, and FOXO. These computational predictions were subsequently validated through molecular docking, which demonstrated stable and high-affinity binding between the primary bioactive constituents of Curcuma and the prioritized target proteins.

Similarly, in a study investigating the Tangshen formula-a Traditional Chinese Medicine (TCM) prescribed for diabetic nephropathy-network pharmacology revealed a set of central targets, including TP53, PTEN, AKT1, BCL2, BCL2L1, PINK1, PARKIN, LC3B, and NFE2L2, alongside associated growth-modulating pathways. Subsequent molecular docking simulations provided structural corroboration by confirming favorable binding interactions between the herbal compounds and these key targets, thereby reinforcing the mechanistic hypotheses generated from the network-based analysis.

This study implements a comprehensive strategy that integrates network pharmacology, computational analysis, synthesis of organic compounds and laboratory experiments to examine the influence of salicylic hydrazide derivatives on tyrosine kinase pathways. A novel aspect of the methodology involves the application of skyline queries, a computational technique from optimization theory, to systematically identify and prioritize significant protein targets within interaction networks (Fatriani et al., 2024). These prioritized targets were then used to screen the potential activity of the compounds. By utilizing these methodologies, we aim to provide a comprehensive understanding of the mechanisms through which these compounds exert their anticancer effects. Insights gained from this research could contribute to the development of new therapeutic strategies targeting tyrosine kinases, ultimately improving treatment outcomes for cancer patients.

2. EXPERIMENTAL SECTION

2.1 Materials

All chemicals used in this study were commercially sourced from certified suppliers. The synthesis of salicylic hydrazide derivatives was carried out using a domestic microwave oven SANYO EM-S2612S as the heating source. The ^{1}H- and ^{13}C-NMR spectra of the synthesized compounds were recorded on a Bruker Ultrashield 600 spectrometer operating at 600 MHz and 150 MHz, respectively. Molecular mass analysis was performed in ESI mode. Melting points were determined with an Electrothermal apparatus without correction. For the biological assays, absorbance measurements were obtained with a 2300 EnSpire Multimode Plate Reader (PerkinElmer, Inc.) at a wavelength of 540 nm. Network pharmacology analysis was done using Cytoscape 3.10.3 and molecular docking was done using Molecular Operating Environment 2022 software from Chemical Computing Group.

2.2 Methods

2.2.1 Construction of Molecule-Target-Pathway Network

Protein targets predicted to interact with the nine tested compounds were obtained from Swiss Target Prediction (http://www.swisstargetprediction.ch/), using Homo sapiens as the reference species. Tyrosine kinase-related proteins were retrieved from the UniProt database (https://www.uniprot.org/). All identified targets across the compounds were subsequently consolidated to construct the Molecule-Target Interaction network.

2.2.2 Construction of Protein-protein Interaction (PPI) Network

The targets associated with the nine salicylic hydrazide derivatives from the preceding step were merged, and a protein– protein interaction (PPI) network was generated using STRING (https://string-db.org). The PPI search was performed using the full STRING network option with a high-confidence threshold of 0.700. The resulting interaction data were subsequently imported into Cytoscape for further evaluation. Prior to analysis, isolated subgraphs lacking connections to the primary network were removed. Network characterization was conducted using the CentiScape 2.2 plugin, producing centrality metrics that included Degree, Betweenness, Closeness, Bridging, and Radiality (Scardoni et al., 2014).

2.2.3 Identifying Protein Targets Through a Skyline-Based Query

Skyline queries are used to filter out a set of interesting data points from a large dataset based on multiple criteria, effectively excluding dominated data points and retaining only the most relevant ones (Torres-Avilés et al., 2024). This method is particularly useful in handling large and complex datasets. In this study, skyline query was used to determine the most significant targets in protein-protein interaction network based on their centrality (Fatriani et al., 2024). According to the skyline concept, a significant protein in an interaction network is classified as a non-dominant protein. Protein X is said to dominate another protein Y if X has equal or better values in all degree centrality measures and is superior in at least one of them. A skyline query retrieves a set of proteins that are not dominated by any other. Skyline query was implemented using block-nested loop algorithm to compare and identify non-dominated targets.

2.2.4 Enrichment Analysis

Enrichment analysis was performed to identify the targets that associated with cancer and tyrosine kinase using Gene ontology and KEGG pathways. Gene ontology is divided into three: molecular functions, biological process, and cell component. Molecular function explains how the genes work in the molecular level. Biological processes explain how the genes contribute in biological processes, and cell component provide the genes location in the cell (Ashburner et al., 2000). KEGG pathway (Kyoto Encyclopedia of Gene and Genomes) show what the disease of disorder the genes are contributes to. Enrichment analysis was performed by analyzing gene Ontology (GO) and KEGG Pathways. Enrichment analysis was performed using a web-based application EnrichR (Xie et al., 2021). The top GO and KEGG pathways are visualized using a dot plot using SRPlot (bioinformatics.com.cn/srplot).

2.2.5 Synthesis of Salicylic Hydrazide Derivatives

S1 was synthesized by reacting methyl salicylate with hydrazine hydrate (2 eq) by microwave irradiation at 120 W for 8 minutes via a nucleophilic acyl substitution mechanism. The reaction mixture was then quenched with water to remove excess hydrazine hydrate, filtered, and the resulting solid was purified through recrystallization. Subsequently, S2–S6 were produced by reacting S1 with various benzoyl chlorides (1 eq) dissolved in THF at 5°C, and the mixture was stirred for 5–35 minutes until completion, as monitored periodically by TLC. Meanwhile, S7–S9 were obtained by reacting S1 with substituted benzaldehydes dissolved in THF under microwave irradiation at 320–360 W for 2 minutes. All reaction products were purified by recrystallization using appropriate solvents.

2.2.6 Inhibition Assay on Human A549 Lung Cancer Cell Growth

The bioassay against the human lung cancer A549 cell line was performed using cultures maintained in an enriched medium composed of Dulbecco's Modified Eagle Medium (DMEM), 10% heat-inactivated fetal bovine serum (FBS), amphotericin B, and kanamycin. Three-day-old cells were used for the assay. A mixture of 1 μL of each sample (1% in DMSO) and 99 μL of A549 cells (5×10^3 cells) was incubated at 37°C for 72 hours. Following the treatment procedure, the absorbance was measured at 540 nm using a Multimode Plate Reader. Cell growth inhibition was calculated using the following equation:

$$\%\,\text{Inhibition} = \left[1 - \frac{A_{\text{sample}} - A_{\text{blank}}}{A_{\text{control}} - A_{\text{blank}}}\right] \times 100 \qquad (1)$$

The IC_{50} value was defined as the sample concentration required to inhibit 50% of cancer cell proliferation. IC_{50} values are presented as mean ± SD from three independent replicates. A lower IC_{50} value relative to the standard drug (doxorubicin) indicates higher cytotoxic activity against A549 cancer cells (Sulistyowaty et al., 2020, 2021).

2.2.7 Molecular Docking

The computer hardware specification used for molecular docking study is Intel®Core™i5-10400F @ 2.90 GHz processor (CPU), with Nvidia®GeForce GTX 1650 as graphic processing unit, and 16 GB Random Access Memory (RAM) with Windows 10 Pro 64-bit. For dynamic simulation, the computer specifications used were Intel Core i9-12900F processor with Nvidia RTX 3080Ti as the graphic processing unit, and a 128 GB Random Access Memory (RAM).

The three-dimensional structure of SRC was obtained from the Protein Data Bank using PDB ID 4MXX (Levinson and Boxer, 2014). Molecular docking was carried out with the Molecular Operating Environment (MOE) 2022 software provided by Chemical Computing Group. The workflow started with method validation, which consisted of redocking the native ligand into its original binding pocket and verifying the procedure through the Root Mean Square Deviation (RMSD) value. After successful validation, the test compounds were docked using the same established protocol. Binding affinity was assessed through the MOE docking score, "S." Furthermore, amino acid interaction profiles were examined using the 2D interaction analysis features in BIOVIA Discovery Studio.

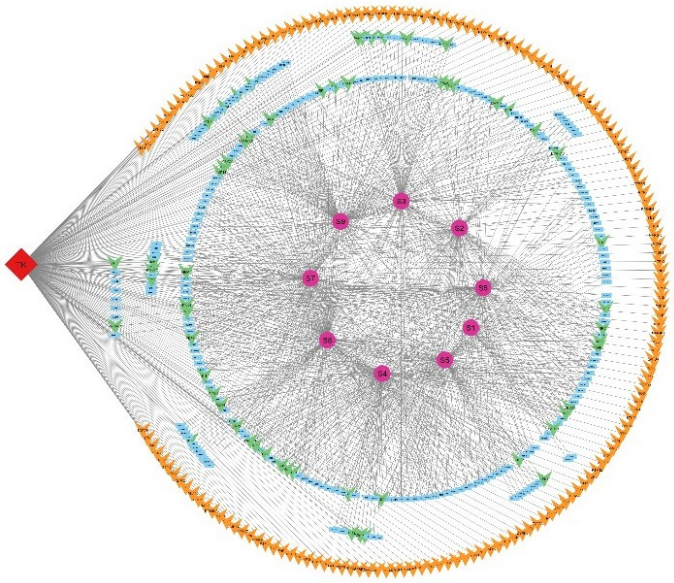

Figure 1. Compounds-Targets-Pathway Interaction Network (Purple: Compound 1 to 9; Blue: Compound's Targets That Not Contributes to TK; Green: Compound's Targets That Contributes to TK); Orange: Tyrosine Kinase Targets; Red: Tyrosine Kinase

3. RESULTS AND DISCUSSION

3.1 Network Pharmacology

The target obtained from Uniprot were 310 targets, and the targets associated with salicylic hydrazide derivatives obtained from STRING were 810. Protein interactions related to Ty-

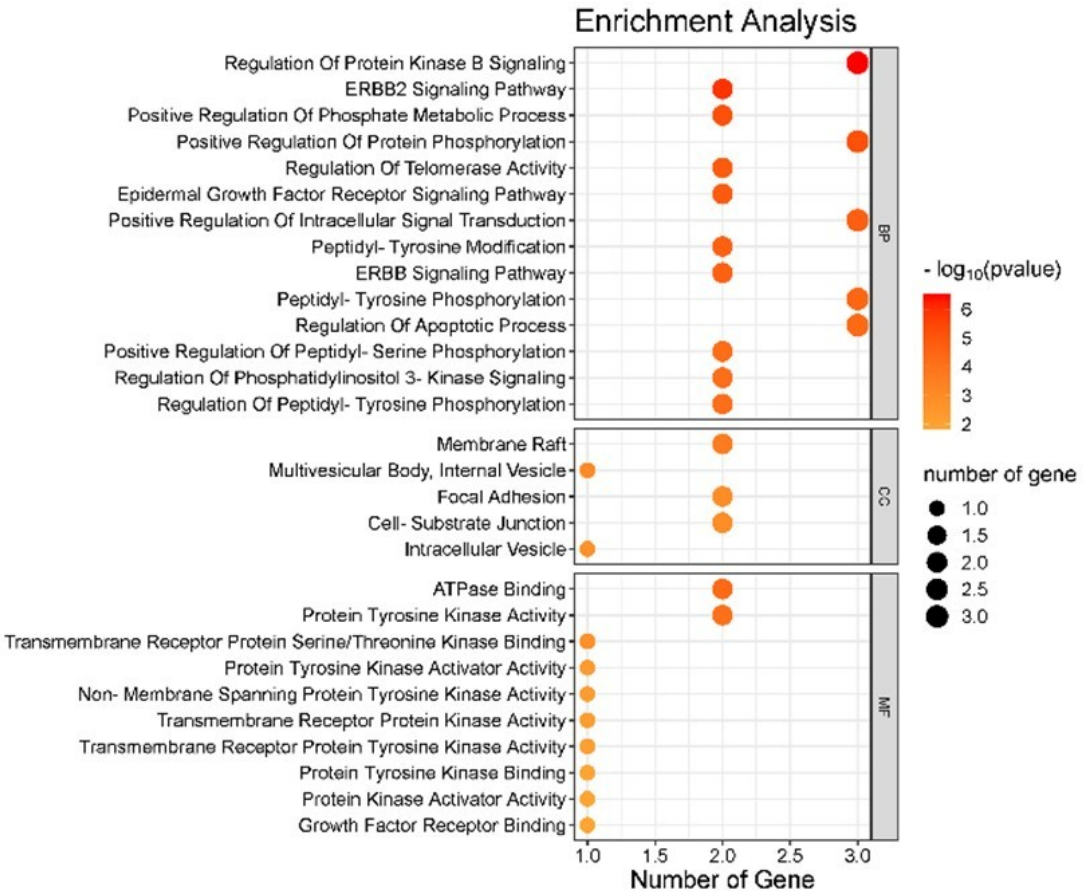

Figure 2. Top Gene Ontologies Based on The Lowest *p*-Value

rosine kinase included 259 proteins with 1062 interactions. Compound-targets network involves 303 proteins with 813 interactions. Both networks were subsequently merged, and any redundant entries were eliminated. The elimination of the duplicates resulted in a compound-targets-pathway network with 466 proteins with 1035 interaction. The compounds-targets-pathway network is shown in Figure 1.

3.1.1 Identifying Protein Targets Through a Skyline-Based Query

Network analysis started with the formation of Protein-protein interaction of the proteins that predicted to interact with Salicylic hydrazide derivates. Network analysis in the form of centrality measures consists of degree. Closeness, betweenness, Eigenvector, and radiality centralities. To choose the most significant protein, we used the skyline query technique to obtain the most dominant proteins from the graph. The Skyline query output indicated that the three most prominent proteins were HSP90AA1, Epidermal Growth Factor EGFR, and Proto-oncogenic tyrosine-protein kinase (SRC), as shown in Table 1. EGFR and SRC are two of the three receptors identified through the Skyline query that are widely utilized as therapeutic targets in oncology. EGFR is a transmembrane receptor tyrosine kinase that regulates cell proliferation, survival, and differentiation; its aberrant activation is implicated in multiple malignancies, and it is clinically targeted by agents such as erlotinib or gefitinib (Sigismund et al., 2018; Mondal et al., 2023). SRC, in contrast, is a non-receptor tyrosine kinase that modulates signaling pathways controlling tumor growth, invasion, and metastasis; it is therapeutically targeted by inhibitors such as dasatinib, which suppresses SRC-mediated oncogenic signaling (Araujo and Logothetis, 2010; Martellucci et al., 2020).

3.1.2 Enrichment Analysis

Enrichment analysis using Gene Ontology (GO) and KEGG pathways is a core bioinformatics approach for interpreting large gene or protein datasets by identifying biologically meaningful patterns (Carbon et al., 2021). GO enrichment categorizes genes into structured ontologies-Biological Process, Molecular Function, and Cellular Component-to determine which functional themes are statistically overrepresented in a dataset relative to the genome background. KEGG pathway enrichment, meanwhile, maps gene sets to curated signaling and metabolic pathways, enabling the identification of dysregulated biological routes such as cell cycle regulation, apoptosis,

Table 1. The Most Significant Targets According to Skyline Query Result

Target	Degree	Closeness	Betweenness	EigenVector	Radiality
HSP90AA1	52.0	0.001733	7099.77	0.2611	7.7635
EGFR	48.0	0.001751	7077.886	0.2599	7.7868
SRC	43.0	0.001652	4464.160	0.2420	7.6550

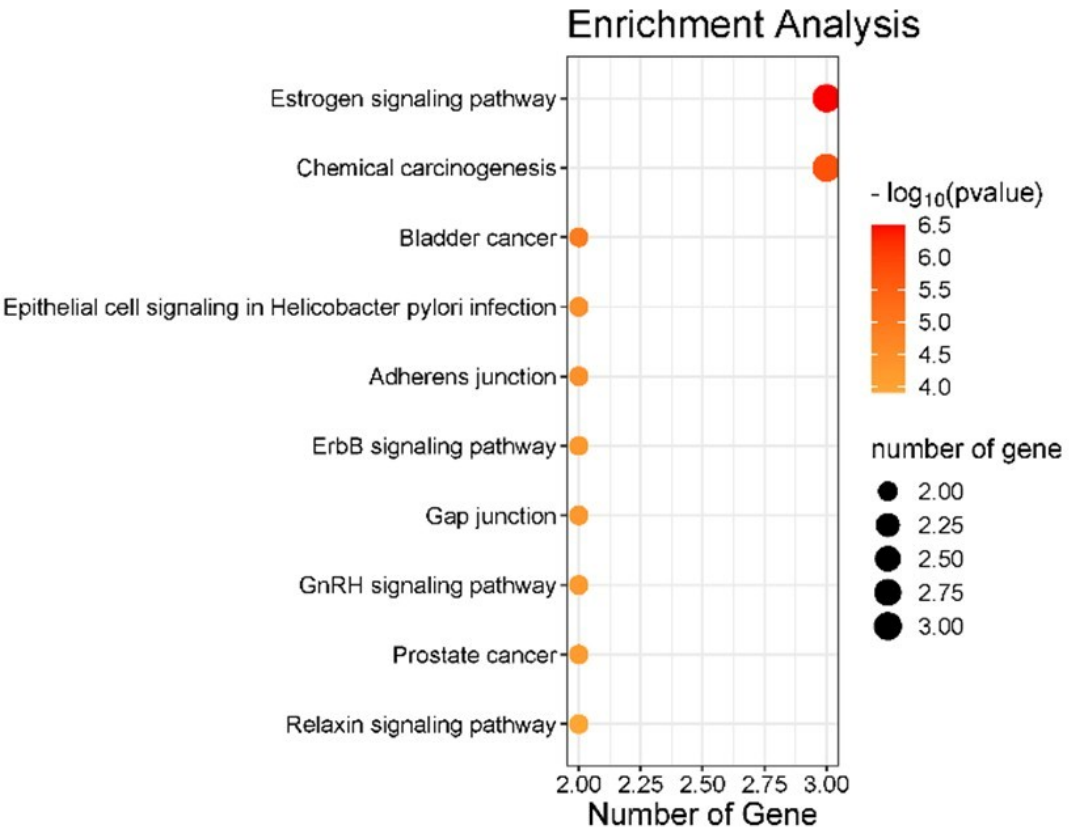

Figure 3. Top KEGG Pathways Based on The Lowest *p*-Value

or metabolic reprogramming (Kanehisa et al., 2023). Together, GO and KEGG enrichment analyses transform raw gene lists into interpretable biological insights, highlighting key processes, molecular functions, and pathways that may underlie a particular phenotype, disease state, or experimental condition.

Enrichment analyses of HSP90AA1, EGFR and SRC were performed using Gene ontology and KEGG Pathway databases. Gene ontology obtained from the 3 targets above included 256 biological processes, 38 for each of cellular component and molecular function. Based on GO biological process, the three proteins were found to play a lot of roles in cancer progression such as regulating protein kinase signal, regulating protein phosphorylation, intercellular signal transduction and peptidyl-tyrosine phosphorylation. EGFR and SRC themselves also play in certain role in cancer progression such as regulating telomerase activity, ERBB and ERBB2 signaling pathway, and most importantly epidermal growth receptor signaling pathway.

Cellular component analysis found that the presence of the three proteins in the membrane raft, focal adhesion and intracellular vesicle. Molecular function analysis showed that these three proteins are contribute in the function of a lot of protein kinase activity, protein tyrosine kinase activities and growth factor receptor binding. The top gene ontologies based on their *p*-value can be seen in Figure 2.

KEGG pathway analysis from these 3 proteins found 75 pathways. Based on the result, HSP90AA1, EGFR and SRC contributes in estrogen signaling pathway and chemical carcinogenesis. According to KEGG pathways, SRC and EGFR contribute in a lot of cancer pathways and types, such as bladder cancer, ErbB signaling pathway, and GnRH signaling pathway. Top KEGG pathways based on their p-value can be seen in Figure 3.

Network pharmacology facilitates the prediction of interactions among target proteins, therapeutic compounds, and their relevance to a specific disease. In this study, a network pharmacology framework supported by a Skyline query was employed

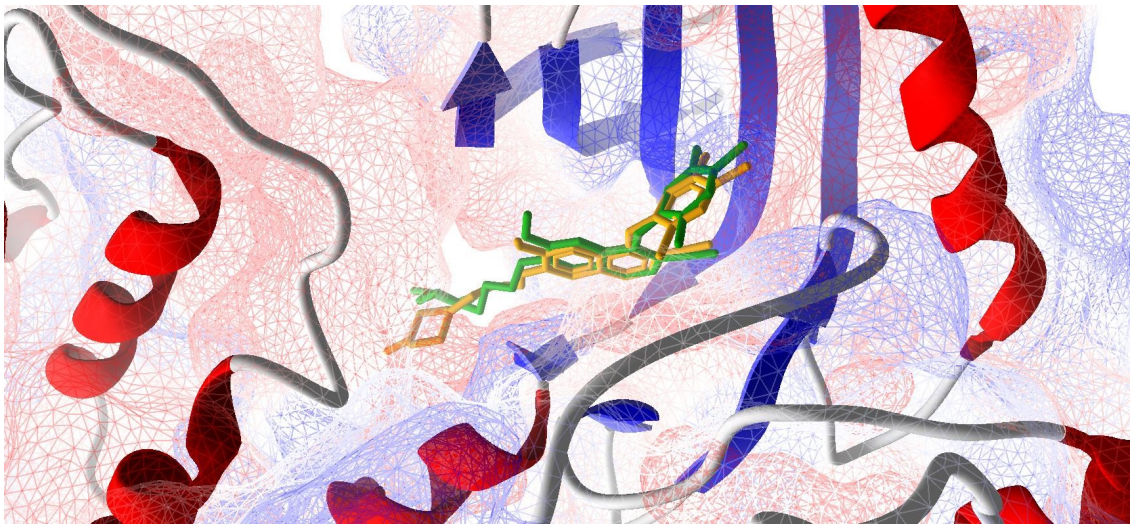

Figure 4. The Superimposition of Native Ligand (Yellow) and the Docked Ligand (Green)

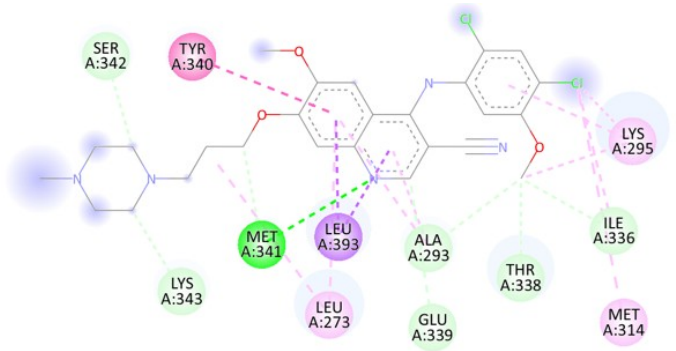

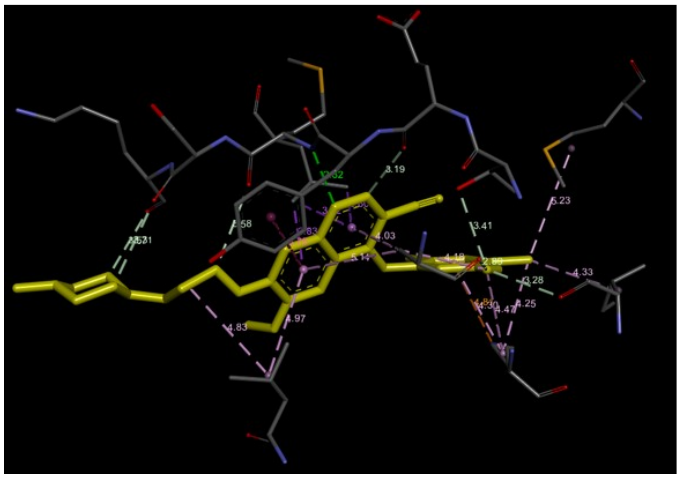

Figure 5. 2D and 3D Structure of Interaction of Bosutinib with SRC

to identify the key proteins within the compound-derived protein network and to assess their linkage to the tyrosine kinase signaling pathway. The network pharmacology results show that HSP90AA1, EGFR and SRC show to be the most dominant proteins in the network. But Gene ontology and KEGG pathways show that SRC to be the most associated protein with cancer progression. Therefore, to confirm activity, we conduct a molecular docking study between the most dominant protein SRC with the derivates.

3.2 Synthetic Outcomes of Salicylic Hydrazide Derivatives (S1–S9)

3.2.1 2-Hydroxybenzohydrazide (S1)

Yield: 73%, m.p = 150°C. ^{1}H NMR (600 MHz, DMSO-d_6) δ 4.58 (s, 2H), 6.78-6.85 (m, 2H), 7.32-7.41 (m, 1H), 7.74 (dd, J = 8.0, 1.6 Hz, 1H), 10.00 (s, 1H), 12.44 (s, 1H) (Saha et al., 2010; Zhang et al., 2020).

3.2.2 N'-Benzoyl-2-Hydroxybenzohydrazide (S2)

Yield: 92%, m.p = 262-265°C. ^{1}H NMR (600 MHz, DMSO-d_6) δ 11.95 (s, 1H), 10.69 (d, J = 8.8 Hz, 2H), 8.02 – 7.87 (m, 3H), 7.61 (t, J = 7.4 Hz, 1H), 7.53 (t, J = 7.6 Hz, 2H), 7.50 – 7.45 (m, 1H), 7.02 – 6.94 (m, 2H). 13C NMR (151 MHz, DMSO) δ 167.80, 165.61, 159.33, 134.20, 132.33, 131.99, 128.55 (2C), 128.30, 127.51 (2C), 119.08, 117.42, 114.56). ESIMS (m/z) = 279.0740 $[M+Na]^+$ ($C_{14}H_{12}O_3N_2Na$) (Mihailović et al., 2017; Selaković et al., 2024).

3.2.3 2-Hydroxy-N'-(2-Hydroxybenzoyl) Benzohydrazide (S3)

Yield: 73%, m.p = 296°C. ^{1}H NMR (DMSO-d_6): δ 6.83–7.34 (m, 8H), 10.5 (s, 2H), 10.87 (s, 2H) (Baashen, 2021; Mogilaiah et al., 2011).

3.2.4 2-Chloro-N'-(2-Hydroxybenzoyl) Benzohydrazide (S4)

Yield: 92%, m.p = 203-205°C. ^{1}H NMR (600 MHz, DMSO-d_6) δ 11.97 (s, 1H), 10.79 (s, 1H), 10.66 (s, 1H), 7.96 (dd, J =

7.9, 1.5 Hz, 1H), 7.58 (ddd, J = 14.3, 7.7, 1.2 Hz, 2H), 7.53 (td, J = 7.7, 1.7 Hz, 1H), 7.50 – 7.45 (m, 2H), 7.02 – 6.94 (m, 2H). ^{13}C NMR (151 MHz, DMSO) δ 167.40, 165.25, 159.28, 134.37, 134.26, 131.62, 130.52, 129.92, 129.48, 128.39, 127.18, 119.11, 117.41, 114.45. ESIMS (m/z) = 313.0351 $[M+Na]^+$ ($C_{14}H_{11}O_3N_2ClNa$) (Hassan et al., 2008).

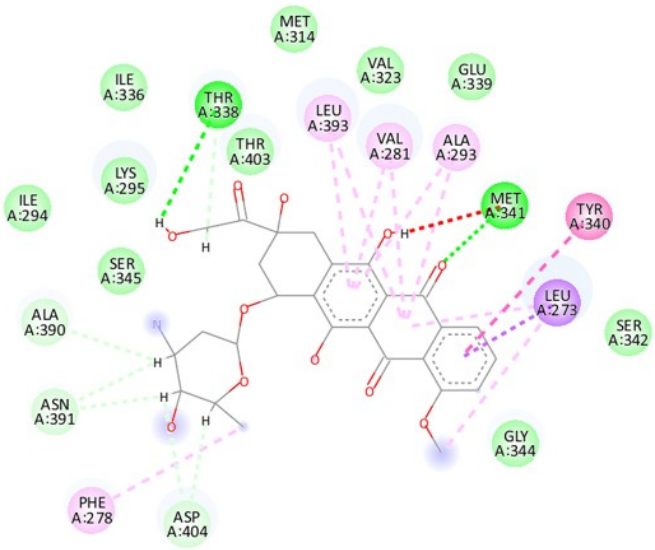

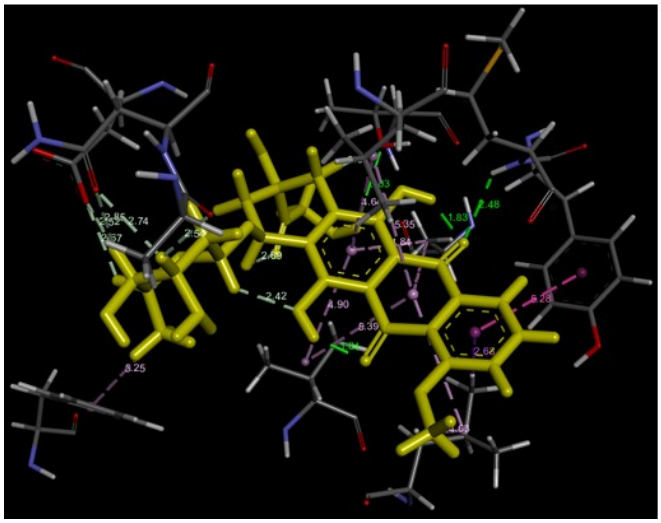

Figure 6. 2D and 3D Structure of Interaction of Doxorubicin with SRC

3.2.5 3,4-Dichloro-N'-(2-Hydroxybenzoyl) Benzohydrazide (S5)

Yield: 90%, m.p = 241- 242°C. ^{1}H NMR (600 MHz, DMSO-d_6) δ 11.83 (s, 1H), 10.91 (s, 1H), 10.72 (s, 1H), 8.16 (d, J = 1.9 Hz, 1H), 7.97 – 7.89 (m, 2H), 7.83 (d, J = 8.4 Hz, 1H), 7.50 – 7.42 (m, 1H), 7.02 – 6.93 (m, 2H). ^{13}C NMR (151 MHz, DMSO) δ 167.36, 163.34, 159.02, 134.90, 134.19, 132.58, 131.56, 131.04, 129.45, 128.51, 127.77, 119.13, 117.36, 114.71. ESIMS (m/z) = 346.9961 $[M+Na]^+$ ($C_{14}H_{10}O_3N_2Cl_2Na$) (Hassan et al., 2008; Zhao and Burke, 1997).

3.2.6 2,4-Dichloro-N'-(2-Hydroxybenzoyl) Benzohydrazide (S6)

Yield: 98%, m.p = 238-241°C. ^{1}H NMR (600 MHz, DMSO-d_6) δ 11.90 (s, 1H), 10.79 (s, 1H), 10.74 (s, 1H), 7.93 (dd, J = 7.9, 1.5 Hz, 1H), 7.76 (d, J = 1.8 Hz, 1H), 7.59 (dd, J = 9.3, 5.0 Hz, 2H), 7.51 – 7.44 (m, 1H), 7.03 – 6.92 (m, 2H). ^{13}C NMR (151 MHz, DMSO) δ 167.14, 164.33, 160.37, 135.41, 134.74, 134.22, 133.19, 131.79, 130.81, 129.50, 128.46, 127.45, 119.12, 117.35, 114.52, 112.79. ESIMS (m/z) = 346.9961 $[M+Na]^+$ ($C_{14}H_{10}O_3N_2Cl_2Na$).

3.2.7 (E)-N'-Benzylidene-2-Hydroxybenzohydrazide (S7)

Yield: 90%, m.p = 250-251°C. ^{1}H NMR (600 MHz, DMSO-d_6) δ 11.85 (s, 2H), 8.47 (s, 1H), 7.90 (d, J = 7.8 Hz, 1H), 7.76 (d, J = 6.5 Hz, 2H), 7.56 – 7.38 (m, 4H), 6.97 (dd, J = 17.7, 8.0 Hz, 2H). ^{13}C NMR (151 MHz, DMSO) δ 164.79, 159.02, 148.73, 134.12, 133.83, 130.29, 128.87 (2C), 128.56, 127.25 (2C), 118.97, 117.28, 115.92. ESIMS (m/z) = 263.0791 $[M+Na]^+$ ($C_{14}H_{12}O_2N_2Na$) (Abdelfattah et al., 2022; Wang et al., 2011).

3.2.8 (E)-2-Hydroxy-N'-(2-Methoxybenzylidene) Benzohydrazide (S8)

Yield: 79%, m.p = 173-174°C. ^{1}H NMR (600 MHz, DMSO-d_6) δ 12.04 (s, 1H), 11.91 (s, 1H), 8.83 (s, 1H), 7.95 – 7.91 (m, 1H), 7.91 – 7.87 (m, 1H), 7.44 (td, J = 8.2, 1.2 Hz, 2H), 7.11 (d, J = 8.4 Hz, 1H), 7.03 (t, J = 7.5 Hz, 1H), 6.98 – 6.91 (m, 2H), 3.87 (s, 3H). ^{13}C NMR (151 MHz, DMSO) δ 165.22, 159.70, 157.92, 144.35, 133.91, 131.86, 128.14, 125.65, 122.07, 120.77, 118.82, 117.38, 115.32, 111.89, 55.70. ESIMS (m/z) = 293.0897 $[M+Na]^+$ ($C_{15}H_{14}O_3N_2Na$) (Abdel-Alim et al., 2005; Singh et al., 1984).

3.2.9 (E)-2-Hydroxy-N'-(4-Hydroxy-3-Methoxybenzylidene) Benzohydrazide (S9)

Yield: 97%, m.p = 210-211°C. ^{1}H NMR (600 MHz, DMSO-d_6) δ 11.72 (s, 3H), 9.59 (s, 2H), 8.35 (s, 3H), 7.90 (d, J = 6.8 Hz, 3H), 7.47 – 7.39 (m, 3H), 7.34 (d, J = 1.4 Hz, 3H), 7.12 (dd, J = 8.1, 1.6 Hz, 3H), 6.95 (dd, J = 16.5, 8.0 Hz, 6H), 6.86 (d, J = 8.1 Hz, 3H), 3.83 (s, 9H). ^{13}C NMR (151 MHz, DMSO) δ 164.64, 159.23, 149.39, 149.27, 148.08, 133.73, 128.36, 125.48, 122.43, 118.88, 117.31, 115.78, 115.49, 109.15, 55.58. ESIMS (m/z) = 309.0846 $[M+Na]^+$ ($C_{15}H_{14}O_4N_2Na$) (Kajal et al., 2022; Terracciano et al., 2018).

The present study demonstrates a clear advancement in both synthetic efficiency and anticancer relevance of compounds S1–S9 compared with structurally related scaffolds reported previously. All compounds were obtained in good to excellent yields (73–98%) using rapid room-temperature or microwave-assisted protocols, representing a substantial improvement over conventional methods that typically require prolonged heating and harsher conditions. Importantly, this work establishes,

for the first time, the cytotoxic potential of several of these scaffolds against A549 lung cancer cells, thereby expanding their pharmacological relevance beyond previously reported non-oncological applications.

Compound S1 showed moderate cytotoxicity (IC_{50} = 218.56 μM) and was synthesized in only 9 min under microwave irradiation, a significant reduction compared with the 9–10 h required in earlier studies (Chaudhary et al., 2010), which did not evaluate anticancer activity. Compound S2 emerged as the most promising candidate, combining high synthetic efficiency (92% yield, 5 min, room temperature) with the strongest cytotoxicity (IC_{50}= 87.65 μM), highlighting this scaffold as a particularly attractive lead for further optimization. This represents a major improvement over previously reported methods that required harsher reagents and lacked anticancer evaluation (Mogilaiah et al., 2011).

Compound S3 exhibited moderate cytotoxicity (IC_{50} = 150.31 μM), contrasting sharply with the weak antioxidant activity reported for related oxadiazoles (Mihailović et al., 2017), indicating that small structural variations and biological context can substantially alter pharmacological behavior. Similarly, compound S4 combined high yield (92%) with moderate cytotoxicity (IC^{50} = 177.38 μM), while requiring significantly shorter reaction times than classical synthetic approaches (Zhao and Burke, 1997), reinforcing the efficiency and practical advantages of the present methodology.

In contrast, compounds S7 and S8 displayed weak to moderate cytotoxicity (IC_{50} = 816.88 and 487.72 μM, respectively), consistent with previous reports that primarily associated these scaffolds with non-cytotoxic functions such as sensing or anti-inflammatory activity. These findings suggest that their structural features may be less favorable for direct anticancer activity, providing valuable preliminary structure–activity relationship insights.

Compound S9 showed moderate cytotoxicity (IC_{50} = 228.40 μM) with excellent synthetic efficiency (97% yield, 2 min), further demonstrating the effectiveness of microwave-assisted synthesis in rapidly accessing biologically relevant heterocycles. Overall, the identification of S2 as the most active compound, together with the consistent improvement in synthetic efficiency across the series, underscores the potential of these scaffolds as promising starting points for the development of novel anticancer agents. These results not only validate the synthetic strategy but also establish a previously unrecognized anticancer profile for this class of compounds.

3.3 Results of Biological Activity and In Silico Studies

To validate the molecular docking protocol, a redocking procedure was conducted by re-docking the co-crystallized ligand into the active site of the target protein. The superimposition of the native ligand (yellow) and the redocked pose (green) resulted in an RMSD value of 1.42 Å, indicating good agreement between the predicted and experimental binding modes. This RMSD value (<2.0 Å) confirms the reliability and accuracy of the docking protocol. The corresponding superimposition figure for validation of the in-silico study is presented in Figure 4.

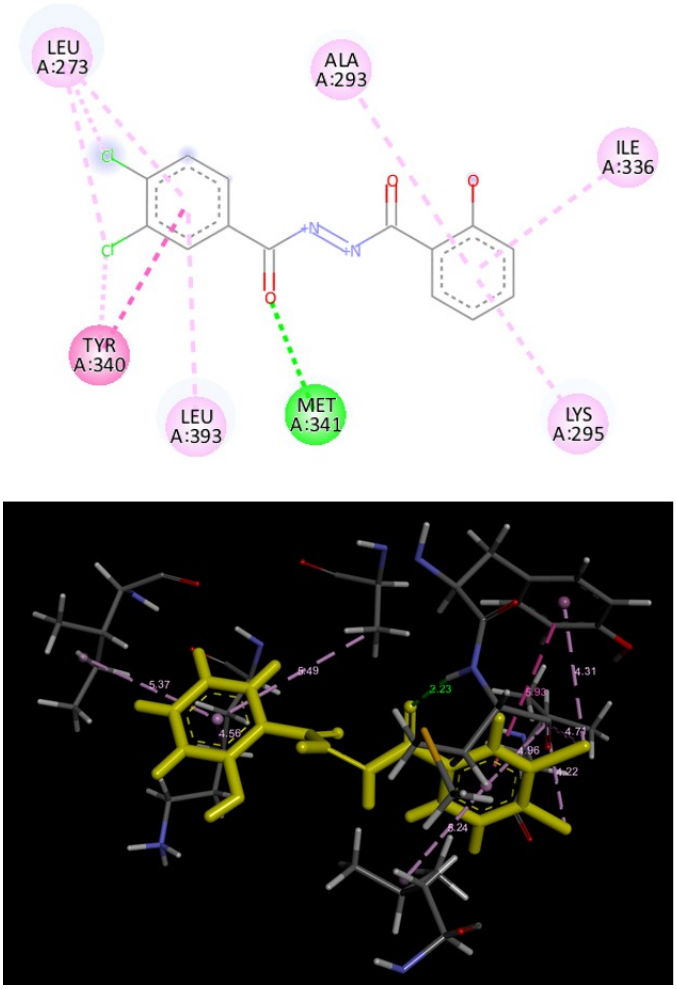

Figure 7. 2D and 3D Structures of S5 Compound Interactions on SRCs

From the docking scores presented in table 2, none of the compounds S1-S9 have a binding energy lower than that of the native ligand in Proto-oncogene tyrosine-protein kinase Src. (PDB ID: 4MXX) which is Bosutinib (-8.73699 kcal/mol). The interaction of Bosutinib with 4MXX involves conventional hydrogen bonds with the amino acid Met341, where the nitrogen atom of Bosutinib is at a distance of 2.82 Å, and carbon hydrogen bonds with the carbon atoms of the amino acids Lys343, Ser342, Ala293, Glu339, Thr338, and Ile336, as illustrated in Figure 5.

Molecular docking results show that the docking score of doxorubicin (-8.4817944 kcal/mol) is higher than that of bosutinib (-8.73699 kcal/mol), indicating that doxorubicin is not significantly better than bosutinib in inhibiting tyrosine kinase. The interactions formed with doxorubicin against SRCs include one conventional hydrogen bond between the aromatic ring of doxorubicin and the amino acid Thr338, as well as four

Table 2. Summary of In Vitro Cytotoxicity Against A549 Cells and Molecular Docking Scores of Salicylic Hydrazide Derivatives

Compound	IC_{50} (μM)	Docking score (kcal/mol)
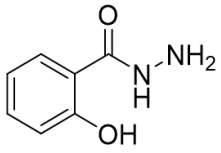 **S1**	218.56 ± 34.03	-4.95215
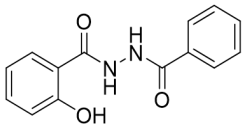 **S2**	87.65 ± 7.96	-6.06909
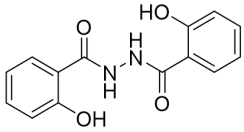 **S3**	150.31 ± 20.72	-6.29493
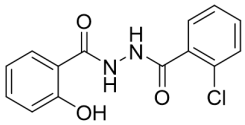 **S4**	177.38 ± 27.81	-6.45701
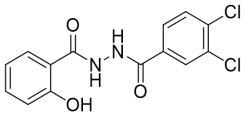 **S5**	68.75 ± 7.25	-6.53468
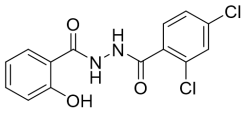 **S6**	93.83 ± 7.63	-6.45659
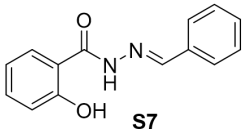 **S7**	816.88 ± 26.24	-5.73763

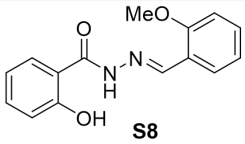 S8	487.72 ± 16.02	-6.49207
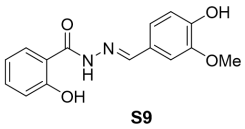 S9	228.40 ± 31.84	-6.2512
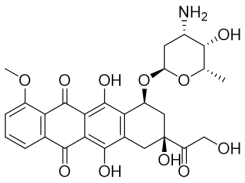 DOX	22.14 ± 4.76	-8.48179
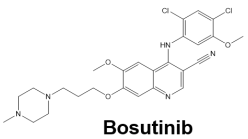 Bosutinib	NA	-8.73699

hydrogen bonds with Ala390, Asn391, Asp404, and Thr338, as depicted in Figure 6.

The compounds S1-S9 have docking scores that are higher, ranging from -8.48179 kcal/mol to -4.95215 kcal/mol. The docking scores for compounds S1-S9 indicate that they are not significantly better than bosutinib and doxorubicin in inhibiting proto-oncogene tyrosine-protein kinase Src. This is consistent with the in vitro anticancer tests on the human lung cancer cell line A459, which showed IC_{50} values greater than that of doxorubicin. The in vitro testing results are divided into two categories: the first category includes inactive anticancer activity (>200 μM) for S1, S2, S4, S7, S8, and S9. The second category includes moderate anticancer activity (20-100 μM) for compounds S3, S5, and S6, as summarized in Table 2.

The in-silico docking analysis showed that compound S5 had a favorable docking score of -6.53468 kcal/mol, suggesting strong binding affinity to tyrosine kinase targets. This result is consistent with the in vitro cytotoxicity data, where S5 exhibited the highest anticancer activity (IC_{50} = 68.75 μM) among the tested compounds. The alignment between computational predictions and experimental results supports the reliability of molecular docking in guiding the selection of promising anticancer candidates. S5 forms one conventional hydrogen bond with Met341 on SRC and six hydrophobic interactions with Leu273, Tyr340, Leu393, Lys295, Ile336, and Ala293 on SRC. This interaction is depicted in Figure 7.

The superior anticancer activity of compound S5 can be largely attributed to the presence of a 3,4-dichloro substitution on the benzoyl ring. Halogen substitution, particularly chlorine, is well known to enhance biological activity by modulating electronic properties, and binding interactions with protein targets. Electron-withdrawing chloro groups can favorably alter the electron density of the hydrazide scaffold, improving ligand–target complementarity and stabilizing key hydrogen-bonding interactions within tyrosine kinase active sites (Hernandes et al., 2010).

In addition, chloro substituents increase molecular lipophilicity, which is often correlated with improved membrane permeability and intracellular target engagement, thereby enhancing anticancer efficacy (Lipinski et al., 2001). From a structural standpoint, chlorine atoms can contribute to hydrophobic and van der Waals interactions within the ATP-binding pocket of tyrosine kinases, and may also participate in directional halogen bonding with electron-rich amino acid residues, further stabilizing the ligand–protein complex (Wilcken et al., 2013). Overall, the enhanced activity of S5 highlights the importance of strategic chloro substitution in optimizing the anticancer potential of salicylic hydrazide derivatives and supports halogenation as a key design strategy in tyrosine kinase–targeted drug discovery.

4. CONCLUSIONS

In conclusion, this study successfully synthesized a series of salicylic hydrazide derivatives (S2–S9) and evaluated their anticancer potential against A549 human lung cancer cells. Integrated network pharmacology and molecular docking identified SRC as a key target, while in vitro cytotoxicity revealed S5 as the most moderated promising compound (IC_{50} = 68.75 μM) with favorable SRC interactions. These findings advance the understanding of salicylic hydrazide scaffolds as tyrosine kinase–targeted anticancer agents. Future studies should focus on structural modification of S5 to enhance potency and selectivity, as well as in vivo evaluation to validate its therapeutic potential.

5. ACKNOWLEDGMENT

The authors gratefully acknowledge the financial support provided by Universitas Airlangga, Surabaya, under the International Research Collaboration Top scheme (Grant No. 1689/UN.LPPM/PT.01.03/2023).

REFERENCES

Abdel-Alim, A.-A. M., A.-N. A. El-Shorbagi, S. G. Abdel-Moty, and H. H. M. Abdel-Allah (2005). Synthesis and Anti-Inflammatory Testing of Some New Compounds Incorporating 5-Aminosalicylic Acid (5-ASA) as Potential Prodrugs. *Archives of Pharmacal Research*, **28**(6); 637–647

Abdelfattah, A. M., A. E. M. Mekky, and S. M. H. Sanad (2022). Synthesis, Antibacterial Activity and in Silico Study of New Bis(1,3,4-oxadiazoles). *Synthetic Communications*, **52**(11–12); 1421–1440

Altıntop, M. D., A. Özdemir, G. Turan-Zitouni, S. Ilgın, Ö. Atlı, G. İşcan, and Z. A. Kaplancıklı (2012). Synthesis and Biological Evaluation of Some Hydrazone Derivatives as New Anticandidal and Anticancer Agents. *European Journal of Medicinal Chemistry*, **58**; 299–307

Araujo, J. and C. Logothetis (2010). Dasatinib: A Potent SRC Inhibitor in Clinical Development for the Treatment of Solid Tumors. *Cancer Treatment Reviews*, **36**(6); 492–500

Ashburner, M., C. A. Ball, J. A. Blake, D. Botstein, H. Butler, J. M. Cherry, and G. Sherlock (2000). Gene Ontology: Tool for the Unification of Biology. *Nature Genetics*, **25**(1); 25–29

Baashen, M. A. (2021). Synthesis of N,N'-Diacylhydrazines and Their Use in Various Synthetic Transformations. *Current Organic Chemistry*, **25**(12); 1394–1403

Carbon, S., E. Douglass, B. M. Good, D. R. Unni, N. L. Harris, C. J. Mungall, and J. Elser (2021). The Gene Ontology Resource: Enriching a GOld Mine. *Nucleic Acids Research*, **49**(D1); D325–D334

Chaudhary, S., P. Chattopadhyay, A. K. Wahi, M. Didel, and V. Dahiya (2010). Synthesis and Study of Antibacterial and Antifungal Activity of Novel 2-(5-Substituted Methylamino-1,3,4-thiadiazol-2-yl)phenols. *Journal of Chemical and Pharmaceutical Research*, **2**(1); 47–52

Fatriani, R., F. A. K. Pratiwi, A. Annisa, D. A. Septaningsih, S. A. Aziz, I. Miladiyah, and W. A. Kusuma (2024). Unveiling the Anti-Obesity Potential of Kemuning (Murraya paniculata): A Network Pharmacology Approach. *PLOS ONE*, **19**(8); e0305544

Hassan, A. A., Y. R. Ibrahim, and A. M. Shawky (2008). Reactions of Substituted Carbohydrazides with Electron-Poor Olefins. *Zeitschrift für Naturforschung B*, **63**(8); 998–1004

Hernandes, M. Z., S. M. Cavalcanti, D. R. Moreira, W. F. de Azevedo Junior, and A. C. Leite (2010). Halogen Atoms in the Modern Medicinal Chemistry: Hints for the Drug Design. *Current Drug Targets*, **11**(3); 303–314

Hopkins, A. L. (2008). Network Pharmacology: The Next Paradigm in Drug Discovery. *Nature Chemical Biology*, **4**(11); 682–690

Kajal, K., G. Singh, T. Pradhan, D. Bhurta, and V. Monga (2022). The Medicinal Perspective of 2,4-Thiazolidinediones Based Ligands as Antimicrobial, Antitumor and Antidiabetic Agents: A Review. *Archiv der Pharmazie*, **355**(9)

Kanehisa, M., M. Furumichi, Y. Sato, M. Kawashima, and M. Ishiguro-Watanabe (2023). KEGG for Taxonomy-Based Analysis of Pathways and Genomes. *Nucleic Acids Research*, **51**(D1); D587–D592

Levinson, N. M. and S. G. Boxer (2014). A Conserved Water-Mediated Hydrogen Bond Network Defines Bosutinib's Kinase Selectivity. *Nature Chemical Biology*, **10**(2); 127–132

Li, L. and S. Kar (2025). Leveraging Network Pharmacology for Drug Discovery: Integrative Approaches and Emerging Insights. *Medicine in Drug Discovery*, **27**; 100220

Lian, L., X.-L. Li, M.-D. Xu, X.-M. Li, M.-Y. Wu, Y. Zhang, and M. Jiang (2019). VEGFR2 Promotes Tumorigenesis and Metastasis in a Pro-Angiogenic-Independent Way in Gastric Cancer. *BMC Cancer*, **19**(1); 183

Lipinski, C. A., F. Lombardo, B. W. Dominy, and P. J. Feeney (2001). Experimental and Computational Approaches to Estimate Solubility and Permeability in Drug Discovery and Development Settings. *Advanced Drug Delivery Reviews*, **46**(1–3); 3–26

Martellucci, S., L. Clementi, S. Sabetta, V. Mattei, L. Botta, and A. Angelucci (2020). Src Family Kinases as Therapeutic Targets in Advanced Solid Tumors: What We Have Learned so Far. *Cancers*, **12**(6); 1448

Mihailović, N., V. Marković, I. Z. Matić, N. S. Stanisavljević, Ž. S. Jovanović, S. Trifunović, and L. Joksović (2017). Synthesis and Antioxidant Activity of 1,3,4-Oxadiazoles and Their Diacylhydrazine Precursors Derived from Phenolic Acids. *RSC Advances*, **7**(14); 8550–8560

Mogilaiah, K., E. Anitha, K. S. Kumar, and R. S. Prasad (2011). A Convenient and Simple Transformation of Acid Hydrazides to N,N'-Diacylhydrazines with $Hg(OAc)_2$ under Solid State Conditions. *ChemInform*, **42**(16)

Mondal, S., S. Vishakha, K. D. Kajal, S. K. Wahan, B. D. Kurmi, and P. Patel (2023). Current Trends in the Development of EGFR Inhibitors as Promising Anticancer Agents:

SAR and Synthetic Studies from (2010–2020). *Current Organic Chemistry*, **27**(1); 2–27

Mutiah, R., M. S. D. Briliana, A. R. A. Ahmad, B. Fauziyah, N. A. Janaloka, and A. Suryadinata (2024). Network Pharmacology and Component Analysis Integrated Study to Uncovers the Molecular Mechanisms of Lansium parasiticum Bark Extract in Colon Cancer Treatment. *Science and Technology Indonesia*, **9**(2); 314–324

Nikolova-Mladenova, B., G. Momekov, Z. Zhivkova, and I. Doytchinova (2023). Design, Synthesis and Cytotoxic Activity of Novel Salicylaldehyde Hydrazones against Leukemia and Breast Cancer. *International Journal of Molecular Sciences*, **24**(8); 7352

Saha, A., R. Kumar, R. Kumar, and C. Devakumar (2010). Development and Assessment of Green Synthesis of Hydrazides. *ChemInform*, **41**(34); 526–531

Scardoni, G., G. Tosadori, M. Faizan, F. Spoto, F. Fabbri, and C. Laudanna (2014). Biological Network Analysis with CentiScaPe: Centralities and Experimental Dataset Integration. *F1000Research*, **3**; 139

Selaković, S., M. V. Rodić, I. Novaković, I. Z. Matić, T. Stanojković, A. Pirković, and M. Šumar-Ristović (2024). Cu(II) Complexes with a Salicylaldehyde Derivative and α-Diimines as Co-Ligands: Synthesis, Characterization, Biological Activity. Experimental and Theoretical Approach. *Dalton Transactions*, **53**(6); 2770–2788

Sigismund, S., D. Avanzato, and L. Lanzetti (2018). Emerging Functions of the EGFR in Cancer. *Molecular Oncology*, **12**(1); 3

Singh, I. P., S. Gurtu, A. Kumar, J. N. Sinha, K. P. Bhargava, and K. Shanker (1984). Antiinflammatory Activities of Compounds Derived from Salicylic and Benzoic Acids. *Archiv der Pharmazie*, **317**(7); 609–614

Sudhesh Dev, S., S. A. Zainal Abidin, R. Farghadani, I. Othman, and R. Naidu (2021). Receptor Tyrosine Kinases and Their Signaling Pathways as Therapeutic Targets of Curcumin in Cancer. *Frontiers in Pharmacology*, **12**; 772510

Sulistyowaty, M. I., G. Putra, T. Budiati, and K. Matsunami (2020). Synthesis, In Vitro Anticancer Activity and In Silico Study of Some Benzylidene Hydrazide Derivatives. *Key Engineering Materials*, **840**; 277–283

Sulistyowaty, M. I., R. Widyowati, G. S. Putra, T. Budiati, and K. Matsunami (2021). Synthesis, ADMET Predictions, Molecular Docking Studies, and In-Vitro Anticancer Activity of Some Benzoxazines against A549 Human Lung Cancer Cells. *Journal of Basic and Clinical Physiology and Pharmacology*, **32**(4); 385–392

Terracciano, S., G. Lauro, A. Russo, M. C. Vaccaro, A. Vassallo, M. De Marco, and I. Bruno (2018). Discovery and Synthesis of the First Selective BAG Domain Modulator of BAG3 as an Attractive Candidate for the Development of a New Class of Chemotherapeutics. *Chemical Communications*, **54**(55); 7613–7616

Torres-Avilés, R., G. Gutiérrez, M. Muñoz, and M. Caniupán (2024). Skyline Query over K2-Tree Compact Data Structure. In *2024 43rd International Conference of the Chilean Computer Science Society (SCCC)*. pages 1–8

Wang, L., W. Qin, X. Tang, W. Dou, and W. Liu (2011). Development and Applications of Fluorescent Indicators for Mg^{2+} and Zn^{2+}. *The Journal of Physical Chemistry A*, **115**(9); 1609–1616

Wilcken, R., M. O. Zimmermann, A. Lange, A. C. Joerger, and F. M. Boeckler (2013). Principles and Applications of Halogen Bonding in Medicinal Chemistry and Chemical Biology. *Journal of Medicinal Chemistry*, **56**(4); 1363–1388

Xie, Z., A. Bailey, M. V. Kuleshov, D. J. B. Clarke, J. E. Evangelista, S. L. Jenkins, and A. Ma'ayan (2021). Gene Set Knowledge Discovery with Enrichr. *Current Protocols*, **1**(3); e90

Zhang, Q., Y. Queneau, and L. Soulère (2020). Biological Evaluation and Docking Studies of New Carbamate, Thiocarbamate, and Hydrazide Analogues of Acyl Homoserine Lactones as Vibrio fischeri-Quorum Sensing Modulators. *Biomolecules*, **10**(3); 455

Zhao, H. and T. R. Burke (1997). Pentafluorophenyl Ester Activation for the Preparation of N,N'-Diaroylhydrazines. *Tetrahedron*, **53**(12); 4219–4230

